

PREPARATION AND MAGNETIC PROPERTIES OF Ni-Cr DOPED STRONTIUM HEXAFERRITE

S. KANAGESAN^a, M. HASHIM^a, T. KALAIVANI^b, I. ISMAIL^a, R. SABBAGHIZADEH^a

^a*Materials Synthesis and Characterization Laboratory (MSCL), Institute of Advanced Technology (ITMA), Universiti Putra Malaysia, 43400 Serdang, Selangor, Malaysia*

^b*Center for material science and Nano Devices, Department of Physics, SRM University, Kattankulathur – 603 203, Tamil Nadu, India.*

The Ni-Cr-substituted M-type Strontium Hexaferrite such as $\text{SrFe}_{12-2x}\text{Ni}_x\text{Cr}_x\text{O}_{19}$, with $x = 0.2, 0.4, 0.6, 0.8$ mol% has been successfully prepared by the sol-gel process. The ferrites were systematically investigated by using powder X-Ray diffractometer (XRD), High Resolution Scanning Electron Microscope (HR-SEM) and Vibrating Sample Magnetometer (VSM). The XRD analysis confirms the single phase and lattice constants (a and c), have been calculated from the XRD data using powderX software. The lattice parameter was found to increase with increasing nickel-chromium concentration. Values of coercivity are found to increase up to the substitution level of $x = 0.0-0.2$ and then decrease slightly while that of saturation decrease continuously with increase in Ni-Cr concentration.

(Received December 24, 2013; Accepted February 19, 2014)

Keywords: sol-gel; scanning electron microscopy (SEM); ceramics; magnetic properties

1. Introduction

M-type $\text{SrFe}_{12}\text{O}_{19}$ (SrM) with magnetoplumbite structure have extensive applications as materials for permanent magnets, high density recording media, telecommunication, magneto optical and microwave devices [1, 2]. The M-type ferrite crystallizes in a hexagonal structure with 64 ions per unit cell on 11 different symmetry sites. The 24 Fe^{3+} atoms are distributed over five distinct sites: three octahedral sites (12k, 2a and 4f2), one tetrahedral (4f1) site and one trigonal bipyramidal site (2b). At high frequencies, hexaferrites are considered superior to other magnetic materials because they have low eddy current loss and high electrical resistivity.

The electrical, dielectric and magnetic properties of hexaferrites depend upon the method of preparation, composition and the distribution of the substituted cations at the five crystallographic sites. The advantage of the chemical route is that it requires only a lower calcination temperature in the crystallization process. The sol-gel method is has many advantages in the chemical route like lower annealing temperature necessary in the crystallization process and the crystal growth of particles is easier to control by varying the heat treatment. Several cations, such as Cr^{3+} , Al^{3+} , Ga^{3+} , In^{3+} and cation combinations such as $\text{La}^{3+}-\text{Co}^{2+}$, $\text{Gd}^{3+}-\text{Co}^{2+}$, $\text{Nb}^{4+}-\text{Zn}^{2+}$, $\text{Ir}^{4+}-\text{Zn}^{2+}$, $\text{Sm}^{3+}-\text{Co}^{2+}$, $\text{Ti}^{4+}-\text{M}^{2+}$ (M=Mn, Ni, Zn, Co) and $\text{Zr}^{4+}-\text{M}^{2+}$ (M=Mn, Ni, Cu and Zn) have been attempted by several researchers [3-9] in order to improve the magnetic and electrical properties of Sr hexaferrite. In this paper, we report the structural changes (Grain size and cell constants) that may occur due to substitution of Ni-Cr and also the effect on the magnetic (saturation magnetization and coercivity) properties of the materials synthesized by the sol-gel method.

*Corresponding author: kanagu1980@gmail.com

2. Experimental details

The polycrystalline M-type hexaferrites having the following formula $\text{SrFe}_{12-x}\text{Ni}_x\text{Cr}_x\text{O}_{19}$, with $x = 0, 0.2, 0.4, 0.6$ and 0.8 were prepared by sol-gel technique starting from metal nitrates and D-Fructose. Calcined powder was compacted in a disc shape and it was subjected to thermal treatments at 1150°C for 3 h. After treatment, the mass and dimensions of the disks were measured to determine the bulk density ($\rho = m/V$). The structural analysis of the pellet was done by X-ray diffraction (XRD) using a Philips diffractometer and $\text{CuK}\alpha$ radiation. The patterns were taken between 20° to 80° with a step of 0.025° . Different parameters such as lattice constants (a and c), are calculated from the XRD data using powder X software. The microstructure of the sintered disc was analyzed using High resolution Scanning Electron Microscope (HE-SEM). A vibrating sample magnetometer (VSM) Lakeshore 7304 was used to measure the magnetic properties of sintered specimen at room temperature with a maximum applied field of 15000 Gauss.

3. Results and discussion

The XRD patterns of sintered $\text{SrFe}_{12-2x}\text{Ni}_x\text{Cr}_x\text{O}_{19}$ samples with $x = 0.0, 0.2, 0.4, 0.6$ and 0.8 are as shown in Fig. 1. The observed diffraction lines were found to correspond to those of the standard pattern (ICSD- 84-1531) of the strontium hexaferrite with no extra line, indicating thereby that the samples have a single phase hexagonal structure and no unreacted constituents were present in these samples. The amount of Ni and Cr substituted in the synthesized materials is found to be less than the actual amount added to the system. The lattice parameters ' a ' and ' c ' show that the values of ' a ' remain almost constant but the values of ' c ' increase by increasing the Ni-Cr content, x , as shown in Table 1. It indicates that the change of the main axis (c -axis) is larger than that of a -axis for the substitution with Zn-Nb ion. This is attributed to larger ionic radii of the dopants viz. Ni^{2+} (0.69 \AA) and Cr^{4+} (0.52 \AA) than that of Fe^{3+} (0.64 \AA). This is in agreement with the fact that all hexagonal ferrites exhibit constant lattice parameter ' a ' and variable parameter ' c ' [10].

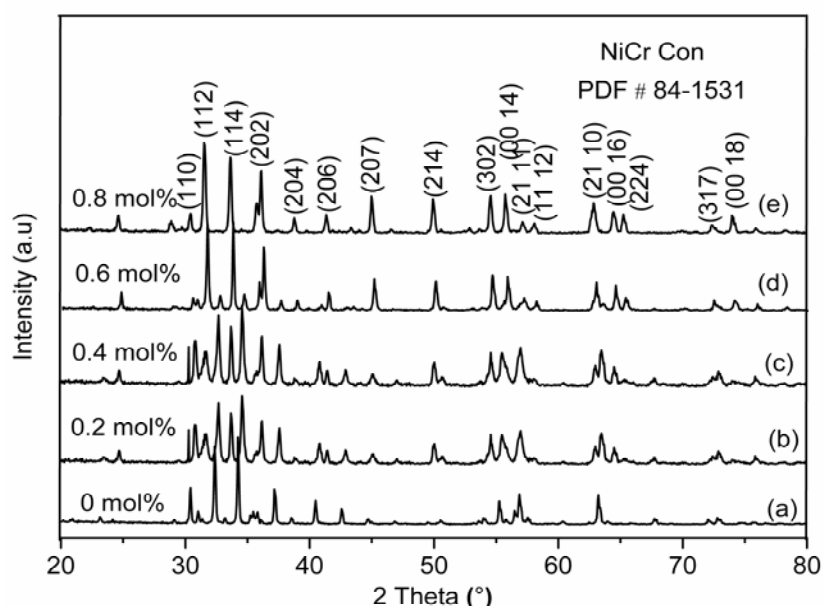


Fig. 1 XRD pattern of samples sintered $\text{BaFe}_{12-2x}\text{Ni}_x\text{Cr}_x\text{O}_{19}$ with different doping concentration

Table 1 Variation of lattice parameters with Ni-Cr substitution

S. No	Hexaferrites (1150°C)	Lattice parameters a=b	Lattice parameter c	Lattice System
1	$\text{SrFe}_{11.6}\text{Ni}_{0.2}\text{Cr}_{0.2}\text{O}_{19}$	5.88	23.18	Hexagonal
2	$\text{SrFe}_{11.2}\text{Ni}_{0.4}\text{Cr}_{0.4}\text{O}_{19}$	5.88	23.19	
3	$\text{SrFe}_{10.8}\text{Ni}_{0.6}\text{Cr}_{0.6}\text{O}_{19}$	5.89	23.21	
4	$\text{SrFe}_{10.4}\text{Ni}_{0.8}\text{Cr}_{0.8}\text{O}_{19}$	5.89	23.23	

The SEM images of samples containing Ni-Cr ($x = 0.2$ and 0.8) were recorded by HR-SEM. It can be observed that for the sample with $x = 0.8$, the particles have well defined shape and clear boundaries and the surface of the grain seems to be more compact (Fig. 2). The average grain size increases as the substitution increase. The average grain size obviously tends to increase with Ni-Cr content. This suggests that Zn-Nb substitutions encourage the grain growth as confirmed by the HR-SEM micrographs [11]. Same types of grain growth occur in Co and Zr substituted barium strontium hexaferrite [12]. Energy dispersive X-ray (EDX) analysis of $\text{BaFe}_{12-x}\text{Ni}_x\text{Cr}_x\text{O}_{19}$ ($x = 0.8$ mol%) sample shows the evidence for the presence of Ni-Cr in Fig. 2b (inset).

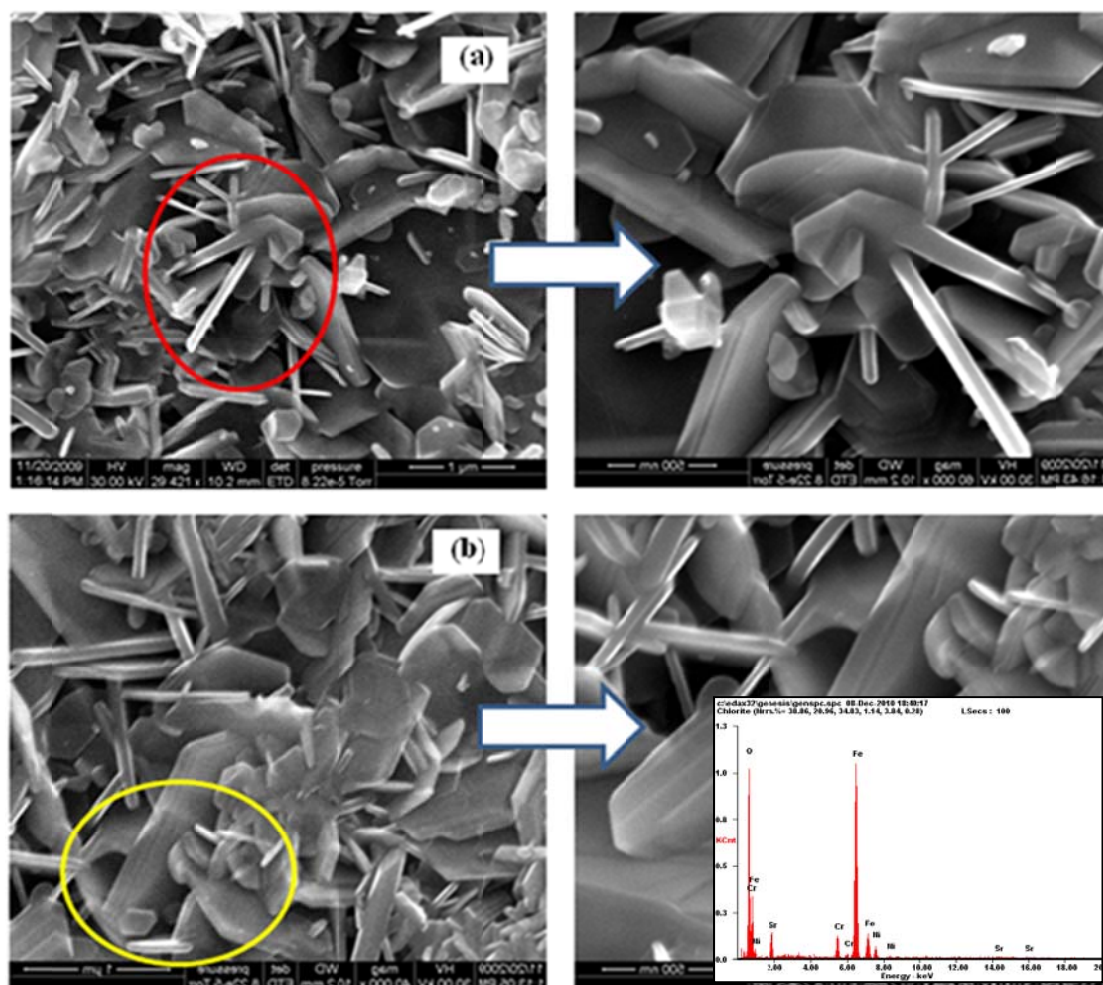


Fig. 2 FE-SEM image of $\text{BaFe}_{12-2x}\text{Ni}_x\text{Cr}_x\text{O}_{19}$ ($x = 0.2, 0.8$ mol%) samples sintered at 1150°C for 3 hours

Magnetism in ferrite originates from the net magnetic moment of ions with spin up and spin down in sublattice sites. The magnetic properties such as saturation magnetization (M_s) and coercivity (H_c) were calculated for all the sintered samples from the hysteresis loops as shown in Fig. 3. The magnetic properties such as saturation magnetization (M_s) 68.57 Am²/kg, 42.31 Am²/kg and coercivity (H_c) 5898.35 Gauss are evaluated for the lower substituted (0.2 mol%) samples from the hysteresis loops as shown in Fig. 3. Clearly, Coercivity increase up to 0.2 and then decrease while Magnetic saturation decreased continuously with increasing Ni-Cr content. The behavior of these properties can be explained on the basis of the occupation of doped cations at different sites in the hexagonal structure of the ferrite.

Ni²⁺ and Cr²⁺ ions occupying different sites in the Fe³⁺ sub lattices based on the previous research report [13]. From this report, Ni²⁺ ions replace Fe³⁺ ions at the 4f2 site for $x \sim 0.1$, and at the 12k site for higher values of substitutions. With increasing Cr content, the saturation magnetizations deduce from law of approach to saturation decrease but coercivities increase. The magnetizations are closely related to distribution of Cr³⁺ ions on each crystallographic site and then magnetic dilution or noncollinear structure (spin canting) with the substitution of Fe³⁺ ions by the lower magnetic moment ions. It is clear that the Cr³⁺ ions distribute on spin up Fe sites known as 12k and 2a. Furthermore, the enhancement of coercivities is due to fine grain sizes.

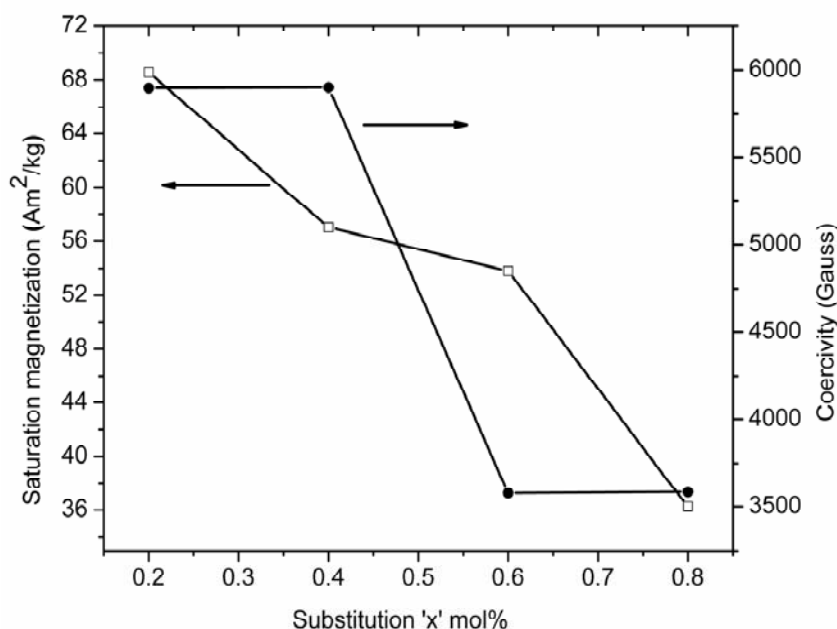


Fig. 3 The specific saturation magnetization (M_s) and the coercivity (H_c) of the samples sintered $BaFe_{12-2x}Ni_xCr_xO_{19}$ as a function of substitution content 'x' mol% at room temperature

4. Conclusion

Hexagonal ferrite $SrFe_{12-x}Ni_xCr_xO_{19}$ was prepared by the sol-gel route and the structure and magnetic properties was investigated. The crystal structure of strontium hexaferrite with small substitutions still remains a hexagonal magnetoplumbite phase. The average size of hexagonal platelets obtained by HR-SEM photographs tends to increase with respect to Ni-Cr content. Changing the substitution rate 'x' mol%, the coercivity could be easily controlled without a significant reduction of M_s at lower substitution level. The results show that the magnetic properties are closely related to the distributions of Ni²⁺-Cr³⁺ ions on the five crystallographic sites. The change in magnetic parameters results in possible use of substituted ferrite for permanent magnet at low level substitution.

Acknowledgements

We would like to thank SRM UNIVERSITY for providing the Nanotechnology center Facilities and ITMA, UNIVERSITI PUTRA MALAYSIA for the pre-submission final editing of this paper.

References

- [1] P. Hernandez, C.D. Francisco, J.M. Munoz, J. Iniguez, L. Torres, M. Zazo, *J. Magn. Magn. Mater.* **157–158**, 123 (1996).
- [2] Z. Jin, W. Tang, J. Zhang, H. Lin, Y. Du, *J. Magn. Magn. Mater.* **182**, 231 (1998).
- [3] M.J. Iqbal, M.N. Ashiq, *Scripta Mater.* **56**, 145 (2007).
- [4] M.J. Iqbal, M.N. Ashiq, P.H. Gomez, J.M. Munoz, *Scripta Mater.* **57**, 1093 (2007).
- [5] M.J. Iqbal, M.N. Ashiq, *Chem. Eng. J.* **136**, 383 (2008).
- [6] M.J. Iqbal, M.N. Ashiq, P.H. Gomez, *J. Alloys Compd.* **478**, 736 (2009).
- [7] N. Shirlcliffe, S. Thompson, E.S.O. Keefe, S. Appleton, C.C. Perry, *Mater. Res. Bull.* **42**, 281 (2007).
- [8] Q.Q. Fang, Y.M. Liu, P. Yin, X.G. Li, *J. Magn. Magn. Mater.* **234**, 366 (2001).
- [9] Chun-Hua Yan, Zhi-Gang Xu, Tao Zhu, Zhe-Ming Wang, Fu-Xiang Cheng, Yun-Hui Huang, Chun-Sheng Liao, *J. Appl. Phys.* **87**, 5588 (2000).
- [10] H. Kojima, in: E.P. Wohlfarth (Eds), *Ferromagnetic materials*, North-Holland, Amsterdam, 1982, pp. 305-391.
- [11] A. Vijayalaksmi, N.S. Gajbhiye, *J. Appl. Phys* **83**, 400 (1998).
- [12] C. Singh, S. Bindra-Narang, I.S. Hudiara, Y. Bai, *J. Alloys Compd.* **464**, 429 (2008).
- [13] M.V. Rane, D. Bahadur, A.K. Nigam, C.M. Srivastava, *J. Magn. Magn. Mater.* **192**, 288 (1999).